

# Adsorption and inhibitive properties for corrosion of carbon steel in hydrochloric acid solution by some nicotinonitrile derivatives

A.A. Al-Sarawy<sup>1</sup>, M.A. Diab<sup>2\*</sup>, A.M. El-Desoky<sup>3</sup>, R.A. El-Bindary<sup>1</sup>

<sup>1</sup>Department of Mathematical and Physical Engineering, Faculty of Engineering, University of Mansoura, Mansoura, Egypt

<sup>2</sup>Department of Chemistry, Faculty of Science, University of Damietta, Damietta 34517, Egypt

<sup>3</sup>Engineering Chemistry Department, High Institute of Engineering & Technology, Damietta, Egypt

**Abstract** – The role of some nicotinonitrile derivatives as corrosion inhibitors for C- steel in 2 M HCl have been studied using weight loss, potentiodynamic polarization, electrochemical impedance spectroscopy (EIS) and electrochemical frequency modulation (EFM) techniques. Polarization studies were carried out at room temperature and showed that all the compounds studied are mixed type inhibitors. The effect of temperature on corrosion inhibition has been studied and the thermodynamic activation and adsorption parameters were calculated to elaborate the mechanism of corrosion inhibition. The morphology of inhibited C- steel was analysed by scanning electron microscope technology with energy dispersive X-ray spectroscopy (SEM-EDX). Electrochemical impedance was used to investigate the mechanism of corrosion inhibition. The presence of these compounds in the solution decreases the double layer capacitance and increases the charge transfer resistance. The adsorption of the compounds on C-steel surface was found to obey Temkin's adsorption isotherm. The mechanism of inhibition process was discussed.

**Keywords** – Adsorption, inhibitive, SEM-EDX, C-steel, HCl.

\*Correspondance Author: E-mail: m.adiab@yahoo.com; Tel.: +2 01005712665; Fax: +2 0572403868

## 1 INTRODUCTION

Acid solutions are widely used in industry, the most important fields of application being acid pickling, industrial acid cleaning, acid decaling and oil well acidizing. Because of the general aggressivity of acid solutions, inhibitors are commonly used to reduce the corrosive attack on metallic materials. Most of the well-known acid inhibitors are organic compounds containing N, O, P, S and aromatic ring or triple bonds. It was reported before that the inhibition efficiency decreases in the order: O < N < S < P [1-4]. In general, organic compounds are effective inhibitors of aqueous corrosion of many metals and alloys. The use of chemical inhibitors to decrease the rate of corrosion processes of carbon steels is quite varied [5-9]. A variety of organic compounds containing heteroatoms such as O, N, S and multiple bonds in their molecule are of particular interest as they give better inhibition efficiency than those containing N or S alone [10,11]. Sulfur and/or nitrogen containing heterocyclic compounds with various substituents are considered to be effective corrosion inhibitors. Hydrazide derivatives offer special affinity to inhibit corrosion of metals in acid solutions [12-15]. Azoles have been intensively investigated as effective steel corrosion [16-21]. The present work aims to characterize the effect of some nicotinonitrile

derivatives as a green corrosion inhibitor of C- steel in 2 M HCl using weight loss measurements and electrochemical methods include potentiodynamic polarization, electrochemical impedance spectroscopy (EIS) and electrochemical frequency modulation (EFM).

## 2 EXPERIMENTAL

### 2.1. COMPOSITION OF MATERIAL SAMPLES

Table (1): Chemical composition (wt %) of the carbon steel.

Chemical constituent	C	Cr	Ni	Si	Mn	P	S	Fe
Composition (wt %)	0.14 - 0.20	0.1	0.01	0.24	0.5	0.05	0.05	rest

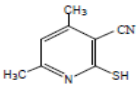
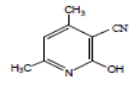
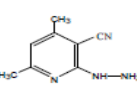
### 2.2. CHEMICALS

#### A- HYDROCHLORIC ACID. (BDH GRADE).

#### B- ORGANIC ADDITIVES

The organic inhibitors used in this study were some nicotinonitrile compounds, listed in the following Table (2).

Table (2): Chemical structures, names, molecular formulas and molecular weights of inhibitors.

Comp. No.	Structure	Name	Mol. Wt. / M. Formula
1		2-Mercapto-4,6-dimethylnicotinonitrile	$C_9H_8N_2S$ 163
2		2-Hydroxy-4,6-dimethylnicotinonitrile	$C_9H_8N_2O$ 147
3		2-Hydrazino-4,6-dimethylnicotinonitrile	$C_9H_{10}N_4$ 133

## 2.3. Methods used for corrosion measurements

### 2.3.1. Weight loss tests

For weight loss measurements, square specimens of size 2 cm x 2 cm x 0.3 cm were used. The specimens were abraded with SiC papers grit sizes (400, 800 and 1200), degreased with acetone l. Then rinsed several times with bidistilled water, and finally dried between two filter papers. The weight loss measurements were carried out in a 100 ml capacity glass beaker placed in a thermostat water bath. The specimens were then immediately immersed in the test solution without or with desired concentration of the investigated compounds. Triplicate specimens were exposed for each condition and the mean weight losses were reported.

### 2.3.2. Potentiodynamic polarization measurements

Polarization experiments were carried out in a conventional three-electrode cell with a platinum counter electrode and a saturated calomel electrode (SCE) coupled to a fine Luggin capillary as the reference electrode. The working electrode was in the form of a square cut from c-steel sheet embedded in epoxy resin of polytetrafluoroethylene so that the flat surface area was 1.0 cm x 1.0 cm. The working electrode was abraded with SiC papers grit sizes up to 1200. Before measurement, the electrode was immersed in solution at natural potential for 30 min. until a steady state was reached.

The potential was started from -500 mV to +500 mV vs.

open circuit potential ( $E_{ocp}$ ). All experiments were carried out in freshly prepared solutions at room temperature and results were always repeated at least three times to check the reproducibility.

### 2.3.3. Electrochemical Impedance Spectroscopy measurements

All EIS measurements were performed at open circuit potential  $E_{ocp}$  at  $25 \pm 1$  °C over a wide frequency range of ( $2 \times 10^{-4}$  Hz to  $8 \times 10^{-2}$  Hz). The sinusoidal potential perturbation was 10 mV in amplitude peak to peak.

### 2.3.4. Electrochemical Frequency Modulation Technique

EFM experiments were performed with applying potential perturbation signal with amplitude 10 mV with two sine waves of 2 and 5 Hz. The choice for the frequencies of 2 and 5Hz was based on three arguments [22]. The larger peaks were used to calculate the corrosion current density ( $j_{corr}$ ), the Tafel slopes ( $\beta_c$  and  $\beta_a$ ) and the causality factors  $CF_2$  and  $CF_3$  [23]. All electrochemical experiments were carried out using Gamry instrument PCI300/4 Potentiostat/Galvanostat/Zra analyzer, DC105 Corrosion software, EIS300 Electrochemical Impedance Spectroscopy software, EFM140 Electrochemical Frequency Modulation software and Echem Analyst 5.5 for results plotting, graphing, data fitting and calculating.

### 2.3.5. SEM-EDX Measurement

The c-steel surface was prepared by keeping the specimens for 3 days in 2M HCl in presence and absence of optimum concentration of some nicotinonitrile derivative, after abraded mechanically using different emery papers up to 1200 grit size. Then, after this immersion time, the specimens were washed gently with distilled water, carefully dried and mounted into the spectrometer without any further treatment. The corroded alloy surfaces were examined using an X-ray diffractometer Philips (pw-1390) with Cu-tube (Cu  $K\alpha_1$ ,  $\lambda = 1.54051$  Å), a scanning electron microscope (SEM, JOEL, JSM-T20, Japan).

### 3. Results and discussion

#### 3.1. Weight loss measurements

Weight loss of C-steel, in  $\text{mg cm}^{-2}$  of the surface area, was determined at various time intervals in the absence and presence of different concentrations ( $1 \times 10^{-6}$  -  $11 \times 10^{-6}$  M) of the some nicotinonitrile derivatives (1-3). The curves obtained in the presence of different concentrations of inhibitors fall significantly below that of free acid as shown in Fig. (1). Similar behaviors were obtained for the other inhibitors (not shown). Values of % IE are tabulated in Table (3). In all cases, the increase in the inhibitor concentration was accompanied by a decrease in the weight loss and an increase in % IE. These results lead to the conclusion that, these compounds under investigation are fairly efficient as inhibitors for C-steel dissolution in HCl solution. Careful inspection of these results showed that, at the same inhibitor concentration, the ranking of the inhibitors according to % IE is as follow:

$$1 > 2 > 3$$

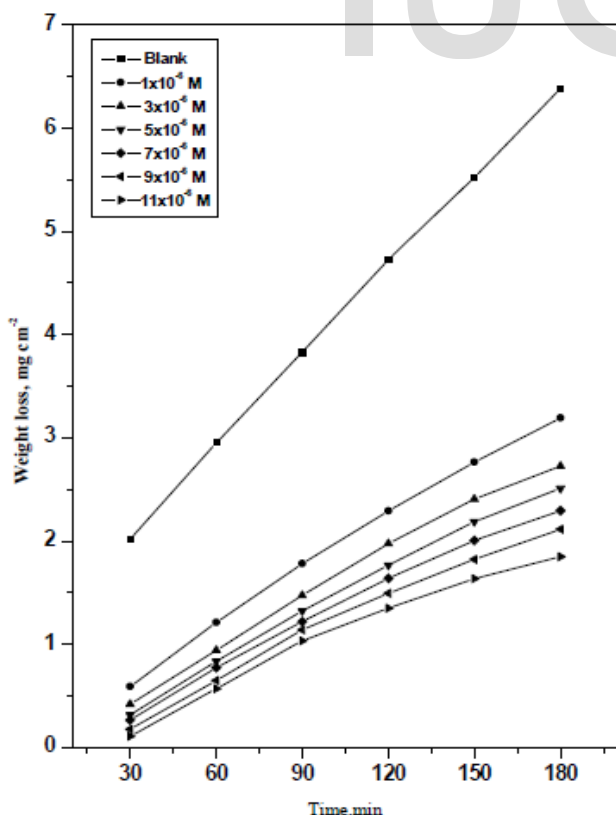


Fig. 1. Weight loss-time curves for the dissolution of C-steel in the absence and presence of different concentrations of compound (1) at 25 °C.

**Table (3):** Variation of inhibition efficiency (% IE) of different compounds with their molar concentrations at 25 °C from weight loss measurements at 120 min. immersion in 2 M HCl.

Conc. (M)	inhibition efficiency (%IE)		
	1	2	3
$1 \times 10^{-6}$	53.4	48.7	46.4
$3 \times 10^{-6}$	61.4	57.0	54.3
$5 \times 10^{-6}$	65.3	60.1	57.5
$7 \times 10^{-6}$	68.0	62.2	59.5
$9 \times 10^{-6}$	70.1	63.8	61.0
$11 \times 10^{-6}$	73.0	67.4	64.5

#### 3.1.1. Adsorption isotherm

Assuming the corrosion inhibition was caused by the adsorption of some nicotinonitrile derivatives, and the values of surface coverage for different concentrations of inhibitors in 2 M HCl were evaluated from weight loss measurement using the following equation:

$$\theta = [\text{weight loss}_{(\text{pure})} - \text{weight loss}_{(\text{inh.})} / \text{weight loss}_{(\text{pure})}] \quad (1)$$

From the values of ( $\theta$ ), it can be seen that the values of ( $\theta$ ) increased with increasing the concentration of some nicotinonitrile derivatives. Using these values of surface coverage, one can utilize different adsorption isotherms to deal with experimental data. The Temkin adsorption isotherm was applied to investigate the adsorption mechanism, by plotting ( $\theta$ ) vs.  $\log C$ , and straight lines were obtained (Fig. 2).

The thermodynamic parameters for the adsorption process that were obtained from this Figure is shown in Table (4). The values of  $\Delta G_{\text{ads}}$  are negative and increased as the % IE increased which indicate that these investigated compounds are strongly adsorbed on the C- steel surface and show the spontaneity of the adsorption process and stability of the adsorbed layer on the C-steel surface. Generally, values of  $\Delta G_{\text{ads}}$  up to  $-20 \text{ kJ mol}^{-1}$  are consistent with the electrostatic interaction between the charged molecules and the charged metal (physical adsorption) while those more negative than  $-40 \text{ kJ mol}^{-1}$  involve sharing or transfer of electrons from the inhibitor molecules to the metal surface to form a coordinate type of bond (chemisorptions) [24]. The values of  $\Delta G_{\text{ads}}$  obtained were approximately equal to  $-40 \pm 1 \text{ kJ mol}^{-1}$ , indicating that the

adsorption mechanism of the some nicotinonitrile derivatives on C- steel in 2 M HCl solution involves both electrostatic adsorption and chemisorptions [25]. The thermodynamic parameters point toward both physisorption (major contributor) and chemisorptions (minor contributor) of the inhibitors onto the metal surface. The  $K_{ads}$  follow the same trend in the sense that large values of  $K_{ads}$  imply better more efficient adsorption and hence better inhibition efficiency [26].

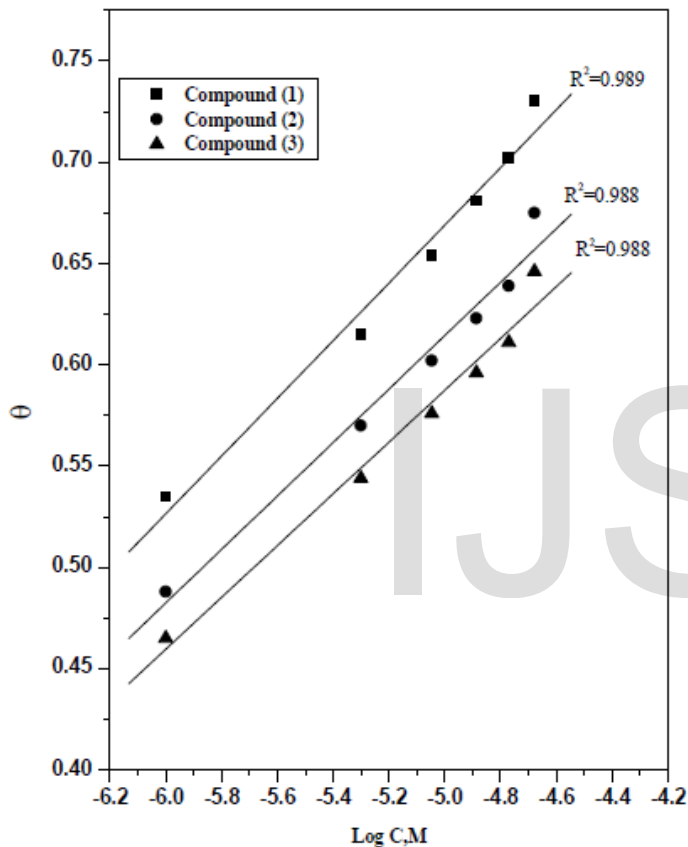


Fig. 2. Temkin adsorption isotherm plotted as  $\theta$  vs.  $\log C$  of the investigated inhibitors for corrosion of C-steel in 2 M HCl solution from weight loss method at 25 °C.

Table (4): Equilibrium constant ( $K_{ads}$ ), adsorption free energy ( $\Delta G^{\circ}_{ads}$ ) for the adsorption of inhibitors on C-steel in 2 M HCl from weight loss method at 25 °C.

Inhibitor	Temkin isotherm	
	$K_{ads} \times 10^{-4} \text{ M}^{-1}$	$-\Delta G^{\circ}_{ads} \text{ kJ mol}^{-1}$
1	495.8	40.3
2	452.7	35.0
3	393.3	33.9

### 3.1.2. Effect of Temperature

Corrosion reactions are usually regarded as Arrhenius processes and the rate ( $k$ ) can be expressed by the relation:

$$\log k = A - \frac{E_a}{2.303 RT} \quad (2)$$

where:  $E_a$  is the activation energy of the corrosion process  $R$  is the universal gas constant,  $T$  is the absolute temperature and  $A$  is a Arrhenius pre-exponential constant depends on the metal type and electrolyte. Arrhenius plots of  $\log k$  vs.  $1/T$  for carbon steel in 2 M HCl in the absence and presence of different concentrations of compound (1) is shown graphically in Fig. (3), similar behaviors were obtained for other compounds. The variation of  $\log k$  vs.  $1/T$  is a linear one and the values of  $E_a$  obtained are summarized in Table (5). These results suggest that the inhibitors are similar in the mechanism of action. The increase in  $E_a$  with the addition of concentration of inhibitors (1-3) indicating that the energy barrier for the corrosion reaction increases. It is also indicated that the whole process is controlled by surface reaction, since the activation energy of the corrosion process is over 20 kJ mol<sup>-1</sup> [27].

Enthalpy and entropy of activation ( $\Delta H^*$ ,  $\Delta S^*$ ) are calculated from transition state theory using the following equation [28]:

$$k = \frac{RT}{Nh} \exp\left(\frac{\Delta S^*}{R}\right) \exp\left(\frac{-\Delta H^*}{RT}\right) \quad (3)$$

Where,  $h$  is Plank's constant,  $N$  is Avogadro's number. A plot of  $\log k/T$  vs.  $1/T$  also gave straight lines as shown in Fig. 4 for carbon steel dissolution in 2 M HCl in the absence and presence of different concentrations of compound (1), similar behaviors were obtained for other compounds. The slopes of these lines equal  $-\Delta H^*/2.303R$  and the intercept equal  $\log RT/Nh + (\Delta S^*/2.303R)$  from which the value of  $\Delta H^*$  and  $\Delta S^*$  were calculated and tabulated in Table (5). From these results, it is clear that the presence of the tested compounds increased the activation energy values and consequently decreased the

corrosion rate of the carbon steel. These results indicate that these tested compounds acted as inhibitors through increasing activation energy of carbon steel dissolution by making a barrier to mass and charge transfer by their adsorption on carbon steel surface. The values of  $\Delta H^*$  reflects the strong adsorption of these compounds on carbon steel surface. The values of  $\Delta S^*$  in absence and presence of the tested compounds are large and negative; this indicates that the activated complex in the rate-determining step represents an association rather than dissociation step, meaning that a decreases in disordering takes place on going from reactants to the activated complex and the activated molecules were in higher order state than that at the initial state [29,30].

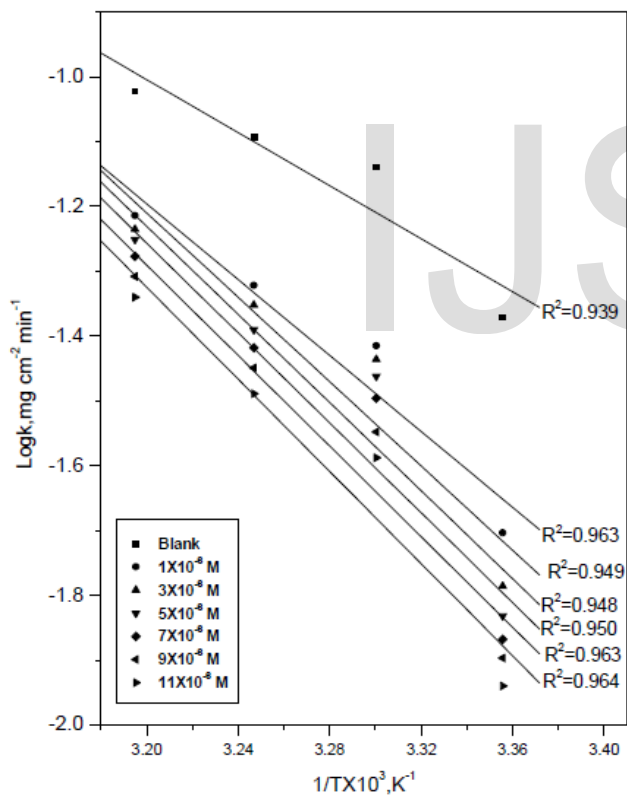


Fig. 3. Arrhenius plots ( $\log k$  vs.  $1/T$ ) for corrosion of C-steel in 2 M HCl in the absence and presence of different concentrations of compound (1).

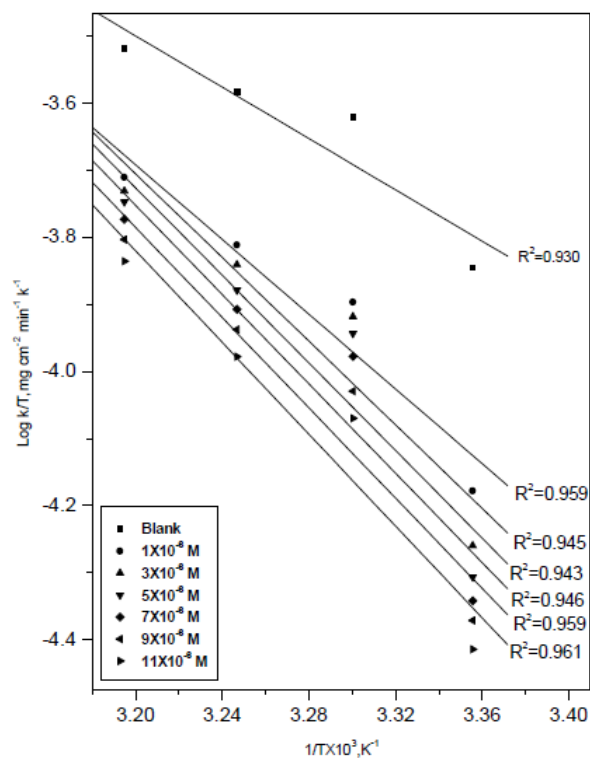


Fig. (4): Plots of ( $\log k / T$ ) vs.  $1/T$  for corrosion of C-steel in 2 M HCl in the absence and presence of different concentrations of compound (1).

Table (5): Thermodynamic activation parameters for the dissolution of C-steel in 2 M HCl in the absence and presence of different concentrations of investigated compounds.

Inhibitor	Conc. M	Ea* kJ mol <sup>-1</sup>	$\Delta H^*$ kJ mol <sup>-1</sup>	S*- $\Delta$ J mol <sup>-1</sup> K <sup>-1</sup>
blank	0.0	38.4	35.6	146.8
1	1x10 <sup>-6</sup>	56.0	53.4	97. 4
	3x10 <sup>-6</sup>	62.3	59.3	77. 3
	5x10 <sup>-6</sup>	65. 1	62.5	67. 7
	7x10 <sup>-6</sup>	66. 3	62. 8	65. 3
	9x10 <sup>-6</sup>	66. 9	64.4	63.80
	11x10 <sup>-6</sup>	68.0	65.5	60. 7
2	1x10 <sup>-6</sup>	52.3	48.7	107.8
	3x10 <sup>-6</sup>	58.1	55.6	90.3
	5x10 <sup>-6</sup>	59.7	57.2	85.9
	7x10 <sup>-6</sup>	59. 9	57.35	85.8
	9x10 <sup>-6</sup>	60.4	57.9	84. 6
	11x10 <sup>-6</sup>	60. 5	58. 3	84.0
3	1x10 <sup>-6</sup>	51.4	48.8	110.8
	3x10 <sup>-6</sup>	56.6	54.0	95. 3
	5x10 <sup>-6</sup>	56.8	54.0	94.9
	7x10 <sup>-6</sup>	57.2	54.7	94.1
	9x10 <sup>-6</sup>	57. 7	55.2	93.4
	11x10 <sup>-6</sup>	58.4	56.1	89. 1



### 3.2. Potentiodynamic polarization

Anodic and cathodic polarizations were carried out potentiodynamic in unstirred 2 M HCl solution in the absence and presence of various concentrations of the inhibitors (1- 3) at 298 K over potential range 300 mV  $\pm$  OCP. The results are represented in Fig. 5 for compound (1), similar behaviors were obtained for other compounds. The obtained potentiodynamic polarization parameters are given in Table (6). These results indicate that the cathodic and anodic curves obtained exhibit Tafel-type behavior. Additionally, the form of these curves is very similar either in the cathodic or in the anodic side, which indicates that the mechanisms of carbon steel dissolution and hydrogen reduction apparently remain unaltered in the presence of these additives. Addition of anhydride compounds decreased both the cathodic and anodic current densities and caused mainly parallel displacement to the more negative and positive values, respectively, i.e. the presence of anhydride derivatives in solution inhibits both the hydrogen evolution and the anodic dissolution processes with overall shift of  $E_{corr}$  to more negative v

vation controlled [32] and the addition of these derivatives did not modify the mechanism of this process. This result suggests that the inhibition mode of the anhydride derivatives used was by simple blockage of the surface by adsorption.

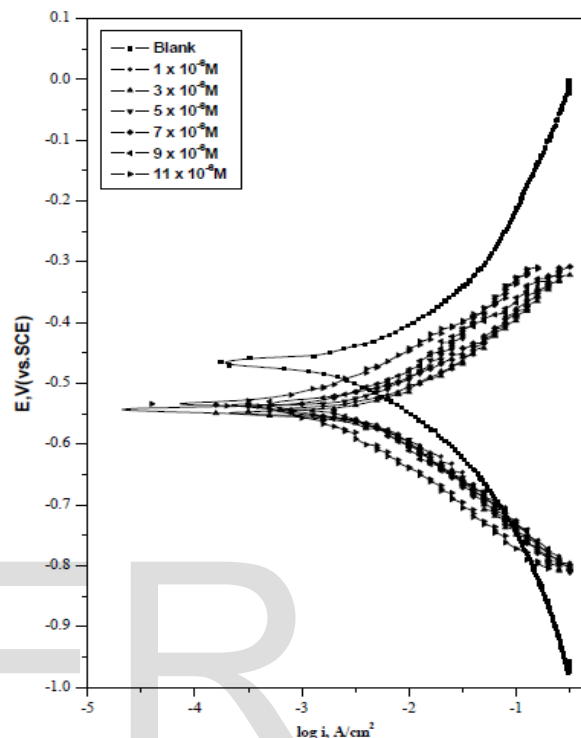


Fig. (5): Potentiodynamic polarization curves for the corrosion of C- steel in 2 M HCl in the absence and presence of various concentrations of compound (1) at 25 °C.

Table (6 ): The effect of concentration of the investigated compounds on the free corrosion potential ( $E_{corr}$ ), corrosion current density ( $i_{corr}$ ), Tafel slopes ( $\beta_a$  &  $\beta_c$ ), inhibition efficiency (% IE), and degree of surface coverage for the corrosion of C- steel in 2 M HCl at 25 °C.

Comp.	Conc., M.	$-E_{corr}$ , mV/(vs SCE)	$i_{corr} \times 10^{-5}$ , $\mu A cm^{-2}$	$\beta_a \times 10^{-3}$ , mV dec <sup>-1</sup>	$\beta_c \times 10^{-3}$ , mV dec <sup>-1</sup>	$\theta$	% IE
1	Blank	500	8.55	85.8	118.5	----	----
	1x10 <sup>-6</sup>	499	1.91	61.6	75.9	0.776	77.6
	3x10 <sup>-6</sup>	496	1.82	53.1	69.5	0.787	78.7
	5 x10 <sup>-6</sup>	472	1.63	36.7	59.0	0.809	80.9
	7x10 <sup>-6</sup>	505	1.58	78.1	85.4	0.815	81.5
	9x10 <sup>-6</sup>	511	1.47	86.4	84.5	0.828	82.8
	11x10 <sup>-6</sup>	516	1.13	88.7	75.7	0.867	86.7
2	1x10 <sup>-6</sup>	489	3.75	81.7	104.8	0.561	56.1
	3x10 <sup>-6</sup>	488	3.51	83.1	113.5	0.589	58.9
	5 x10 <sup>-6</sup>	499	3.12	55.3	75.9	0.635	63.5
	7x10 <sup>-6</sup>	484	2.15	77.0	149.8	0.748	74.8
	9x10 <sup>-6</sup>	491	2.10	68.5	117.2	0.754	75.4
	11x10 <sup>-6</sup>	495	2.08	60.1	76.4	0.756	75.6
3	1x10 <sup>-6</sup>	490	6.00	86.8	116.4	0.298	29.8
	3x10 <sup>-6</sup>	501	5.59	82.6	124.3	0.346	34.6
	5 x10 <sup>-6</sup>	499	4.83	75.2	122.5	0.435	43.5
	7x10 <sup>-6</sup>	495	4.63	80	161	0.458	45.8
	9x10 <sup>-6</sup>	489	4.47	82.1	114.4	0.477	47.7
	11x10 <sup>-6</sup>	509	4.23	74.1	102.2	0.505	50.5

alues with respect to the OCP.

The results also show that the slopes of the anodic and the cathodic Tafel slopes ( $\beta_a$  and  $\beta_c$ ) were slightly changed on increasing the concentration of the tested compounds. This indicates that there is no change of the mechanism of inhibition in presence and absence of inhibitors. The fact that the values of  $\beta_c$  are slightly higher than the values of  $\beta_a$  suggesting a cathodic action of the inhibitor. This could be interpreted as an action of mixed inhibitor control over the electrochemical semi-reactions. This means that the anhydride derivatives are mixed type inhibitors, but the cathode is more preferentially polarized than the anode. The higher values of Tafel slope can be attributed to surface kinetic process rather the diffusion-controlled process [31]. The constancy and the parallel of cathodic slope obtained from the electrochemical measurements indicate that the hydrogen evolution reaction was acti-

### 3.3. Electrochemical Impedance Spectroscopy

Impedance diagram (Nyquist) at frequencies ranging from 1 Hz to 1 kHz with 10 mV amplitude signal at OCP for carbon steel in 2 M HCl in the absence and presence of different concentrations of compounds (1-3) are obtained. The equivalent circuit that describes our metal/electrolyte interface is shown in Fig. 6 where  $R_s$  and  $R_{ct}$  refer to solution resistance and charge transfer resistance, respectively. EIS parameters and % IE were calculated and tabulated in Table (7). In order to correlate impedance and polarization methods,  $i_{corr}$  values were obtained from polarization curves and Nyquist plots in the absence and presence of different concentrations of compounds (1-3) using the Stern-Geary equation:

$$i_{corr} = \frac{\beta_a \beta_c}{2.303 (\beta_a + \beta_c) R_{ct}} \quad (4)$$

The obtained Nyquist plot for compound (1) is shown in Fig. 7. Each spectrum is characterized by a single full semicircle. The fact that impedance diagrams have an approximately semicircular

appearance shows that the corrosion of carbon steel is controlled by a charge transfer process. Small distortion was observed in some diagrams, this distortion has been attributed to frequency dispersion [33]. The diameters of the capacitive loop obtained increases in the presence of some nicotinonitrile derivatives, and were indicative of the degree of inhibition of the corrosion process [34].

It was observed from the obtained EIS data that  $R_{ct}$  increases and  $C_{dl}$  decreases with the increasing of inhibitor concentrations. The increase in  $R_{ct}$  values, and consequently of inhibition efficiency, may be due to the gradual replacement of water molecules by the adsorption of the inhibitor molecules on the metal surface to form an adherent film on the metal surface. And this suggests that the coverage of the metal surface by the film decreases the double layer thickness. Also, this

decrease of  $C_{dl}$  at the metal/solution interface with increasing the inhibitor concentration can result from a decrease in local dielectric constant which indicates that the inhibitors were adsorbed on the surface at both anodic and cathodic sites [35].

The impedance data confirm the inhibition behavior of the inhibitors obtained with other techniques. From the data of Table (7), it can be seen that the  $i_{corr}$  values decrease significantly in the presence of these additives and the % IE is greatly improved. The order of reduction in  $i_{corr}$  exactly correlates with that obtained from potentiostatic polarization studies. Moreover, the decrease in the values of  $i_{corr}$  follows the same order as that obtained for the values of  $C_{dl}$ . It can be concluded that the inhibition efficiency found from weight loss, polarization curves, electrochemical impedance spectroscopy measurements and the Stern-Geary equation are in good agreement.

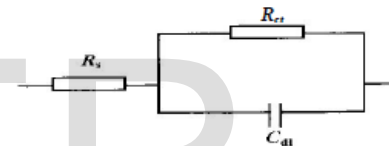


Fig. 6. Electrical equivalent circuit model used to fit the experimental results.

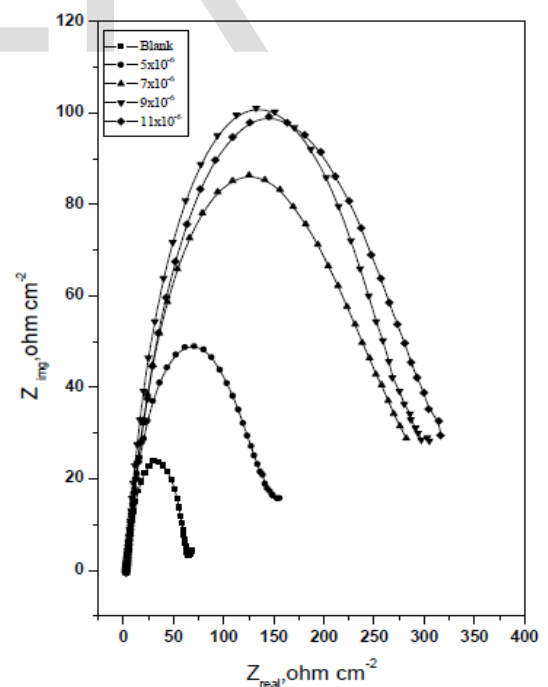


Fig. (7): The Nyquist plots for corrosion of C-steel in 2 M HCl in the absence and presence of different concentrations of compound (1) at 25 °C.

**Table (7):** Electrochemical kinetic parameters obtained by EIS technique for C- steel in 2 M HCl without and with various concentrations of compounds (1 - 3) at 25 °C.

Comp.	Conc.,M .	$Cdl \times 10^{-3}, \mu F cm^{-2}$	$R_{ct}, \Omega cm^2$	$\theta$	%IE
Blank	0.0	6.33	60.9	----	----
1	$5 \times 10^{-6}$	1.19	143.0	0.574	57.4
	$7 \times 10^{-6}$	1.40	268.3	0.773	77.3
	$9 \times 10^{-6}$	5.32	282.7	0.784	78.4
	$11 \times 10^{-6}$	1.21	304.7	0.800	80.0
2	$5 \times 10^{-6}$	9.02	132.2	0.539	53.9
	$7 \times 10^{-6}$	1.32	232.0	0.737	73.7
	$9 \times 10^{-6}$	1.48	272.1	0.776	77.6
	$11 \times 10^{-6}$	1.42	293.9	0.792	79.2
3	$5 \times 10^{-6}$	9.76	81.9	0.256	25.6
	$7 \times 10^{-6}$	8.11	110.0	0.446	44.6
	$9 \times 10^{-6}$	1.36	214.7	0.716	71.6
	$11 \times 10^{-6}$	1.42	239.2	0.745	74.5

### 3.4. Electrochemical Frequency Modulation Technique (EFM)

EFM is a nondestructive corrosion measurement technique that can directly and quickly determine the corrosion current value without prior knowledge of Tafel slopes, and with only a small polarizing signal. These advantages of EFM technique make it an ideal candidate for online corrosion monitoring [36].

The great strength of the EFM is the causality factors which serve as an internal check on the validity of EFM measurement. The causality factors CF-2 and CF-3 are calculated from the frequency spectrum of the current responses. Figure (8) shows the frequency spectrum of the current response of pure carbon steel in 2 M HCl, contains not only the input frequencies, but also contains frequency components which are the sum, difference, and multiples of the two input frequencies. The EFM Intermodulation spectrums of carbon steel in 2 M HCl acid solution containing ( $1 \times 10^{-6}$  M and  $11 \times 10^{-6}$  M) of the studied inhibitors are shown in Figs (9-14). Similar results were recorded for the other concentrations of the investigated compounds (not shown). The harmonic and Intermodulation peaks are clearly visible and are much larger than the background noise. The two large peaks, with amplitude of about 200  $\mu A$ , are the response to the 40 and 100 mHz (2 and 5 Hz)

excitation frequencies. It is important to note that between the peaks there is nearly no current response (<100 nA). The experimental EFM-data were treated using two different models: complete diffusion control of the cathodic reaction and the "activation" model. For the latter, a set of three non-linear equations had been solved, assuming that the corrosion potential does not change due to the polarization of the working electrode [37]. The larger peaks were used to calculate the corrosion current density ( $j_{corr}$ ), the Tafel slopes ( $b_c$  and  $b_a$ ) and the causality factors (CF-2 and CF-3). These electrochemical parameters were simultaneously determined by Gamry EFM140 software, and listed in Table 8. The data presented in Table (8) obviously show that, the addition of any one of tested compounds at a given concentration to the acidic solution decreases the corrosion current density, indicating that these compounds inhibit the corrosion of carbon steel in 2 M HCl through adsorption. The causality factors obtained under different experimental conditions are approximately equal to the theoretical values (2 and 3) indicating that the measured data are verified and of good quality [38]. The inhibition efficiencies  $IE_{EFM} \%$  increase by increasing the studied inhibitor concentrations and was calculated as follows:

$$IE_{EFM} \% = [(1 - i_{corr} / i_{corr}^0)] \times 100 \quad (5)$$

where  $i_{corr}^0$  and  $i_{corr}$  are corrosion current densities in the absence and presence of inhibitor, respectively.

The inhibition sufficiency obtained from this method is in the order:

$$1 > 2 > 3$$

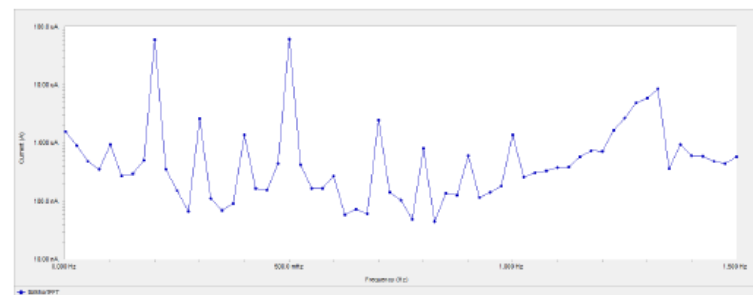


**Fig. 8.** EFM spectra for C-steel in 2 M HCl (blank) at 25 °C.



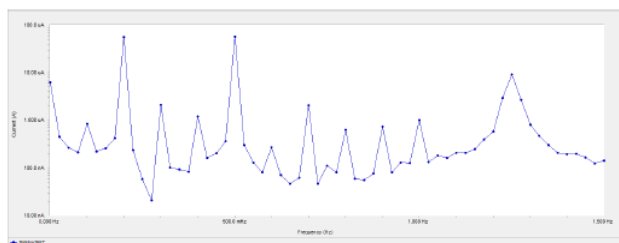


**Fig. 9.** EFM spectra for C- steel in 2 M HCl in the presence of  $1 \times 10^{-6}$  M from compound (1) at 25 °C.

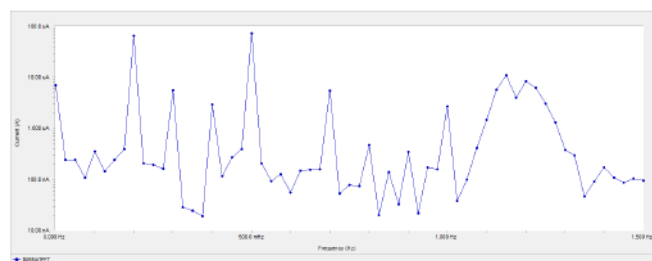


**Fig. 13.** EFM spectra for C- steel in 2 M HCl in the presence of  $9 \times 10^{-6}$  M from compound (1) at 25 °C.

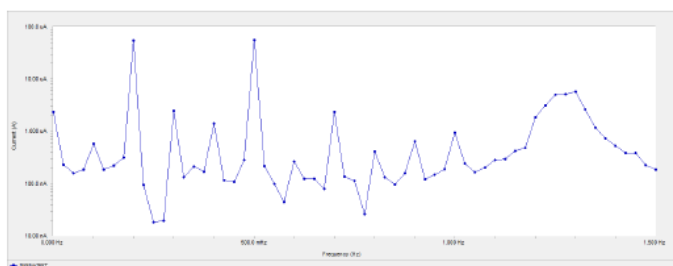


**Fig. 10.** EFM spectra for C- steel in 2 M HCl in the presence of  $3 \times 10^{-6}$  M from compound (1) at 25 °C.

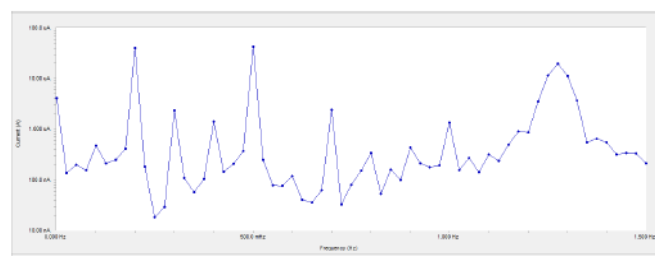


**Fig. 14.** EFM spectra for C-steel in 2 M HCl in the presence of  $11 \times 10^{-6}$  M from compound (1) at 25 °C.

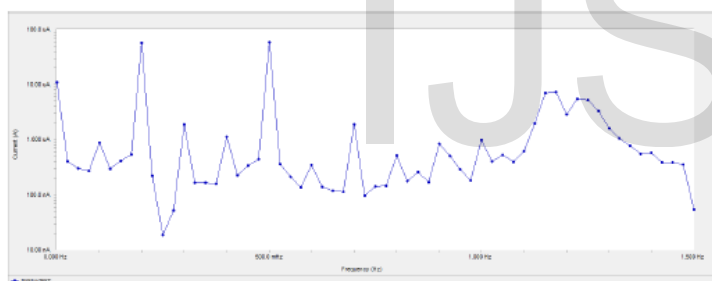


**Fig. 11.** EFM spectra for C- steel in 2 M HCl in the presence of  $5 \times 10^{-6}$  M from compound (1) at 25 °C.

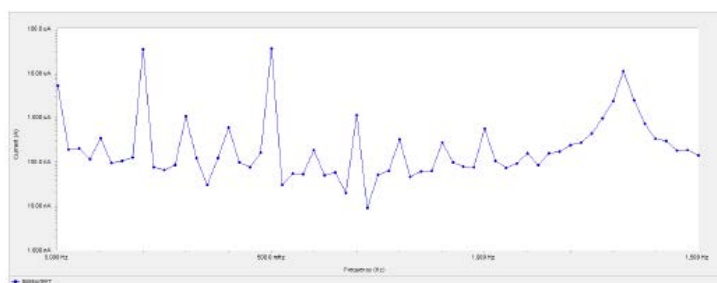


**Fig. 12.** EFM spectra for C- steel in 2 M HCl in the presence of  $7 \times 10^{-6}$  M from compound (1) at 25 °C.

**Table (8):** Electrochemical kinetic parameters obtained by EFM technique for C- steel in 2 M HCl without and with various concentrations of compounds (1 - 3) at 25 °C.

Comp.	Conc., M	$i_{corr.}$ $\mu A\ cm^{-2}$	$\beta_a, \times 10^{-3}$ $mV\ dec^{-1}$	$\beta_c, \times 10^{-3}$ $mV\ dec^{-1}$	CF-2	CF-3	% IE
1	Blank	96.28	91.8	120.6	1.85	2.81	-----
	$1 \times 10^{-6}$	30.69	61.3	76.9	1.96	3.03	68.1
	$3 \times 10^{-6}$	29.27	72.7	98.2	1.83	3.09	69.5
	$5 \times 10^{-6}$	23.07	52.7	58.0	1.65	3.10	76.0
	$7 \times 10^{-6}$	20.04	37.9	44.0	1.86	3.08	79.1
	$9 \times 10^{-6}$	11.84	36.0	41.4	1.70	2.91	87.7
	$11 \times 10^{-6}$	5.621	20.0	21.2	1.99	2.79	94.1
2	$1 \times 10^{-6}$	63.27	62.6	77.0	2.40	3.14	34.2
	$3 \times 10^{-6}$	60.23	97.0	121.8	1.81	2.822	37.4
	$5 \times 10^{-6}$	57.61	63.5	76.6	2.04	3.03	40.1
	$7 \times 10^{-6}$	50.45	74.1	77.25	2.05	2.80	47.6
	$9 \times 10^{-6}$	38.34	88.3	109.5	1.78	3.06	59.8
	$11 \times 10^{-6}$	35.25	64.3	90.2	1.71	2.86	63.3
3	$1 \times 10^{-6}$	91.99	94.4	120.1	1.88	3.04	4.4
	$3 \times 10^{-6}$	79.33	83.1	107.2	2.06	3.08	17.6
	$5 \times 10^{-6}$	70.19	72.5	84.8	1.78	6.365	27.1
	$7 \times 10^{-6}$	69.93	115.0	147.5	1.90	1.815	27.3
	$9 \times 10^{-6}$	68.37	55.3	76.2	1.97	3.11	28.9
	$11 \times 10^{-6}$	68.30	90.1	132.3	1.73	3.21	29.1

### 3.5. Scanning Electron Microscopy (SEM) Studies

Figure (15) represents the micrograph obtained for carbon steel samples in presence and in absence of  $11 \times 10^{-6}$  M some nicotinonitrile derivatives after exposure for 3 days immersion. It is clear that carbon steel surfaces suffer from severe corrosion attack in the blank sample.

It is important to stress out that when the compound is present in the solution, the morphology of carbon steel surfaces is quite different from the previous one, and the specimen surfaces were smoother. We noted the formation of a film which is distributed in a random way on the whole surface of the carbon steel. This may be interpreted as due to the adsorption of the some nicotinonitrile derivatives on the carbon steel surface incorporating into the passive film in order to block the active site present on the carbon steel surface. Or due to the involvement of inhibitor molecules in the interaction with the reaction sites of carbon steel surface, resulting in a decrease in the contact between carbon steel and the aggressive medium and sequentially exhibited excellent inhibition effect [39, 40].

### 3.6. Energy Dispersion Spectroscopy (EDS) Studies

The EDS spectra were used to determine the elements present on the surface of carbon steel and after 3 days of exposure in the uninhibited and inhibited 2 M HCl. Figure 16 shows the EDS analysis result on the composition of carbon steel only without the acid and inhibitor treatment. The EDS analysis indicates that only Fe and oxygen were detected, which shows that the passive film contained only  $\text{Fe}_2\text{O}_3$ .

Figure (16) portrays the EDS analysis of carbon steel in 2 M HCl only and in the presence of  $11 \times 10^{-6}$  M of nicotinonitrile derivatives. The spectra show additional lines, demonstrating the existence of C (owing to the carbon atoms of some nicotinonitrile derivatives). These data shows that the carbon and O atoms covered the specimen surface. This layer is entirely owing to the inhibitor, because the carbon and O signals are absent on the specimen surface exposed to uninhibited HCl. It is seen that, in addition to Mn, C and O were present in the spectra. A comparable elemental distribution is shown in Table (9).

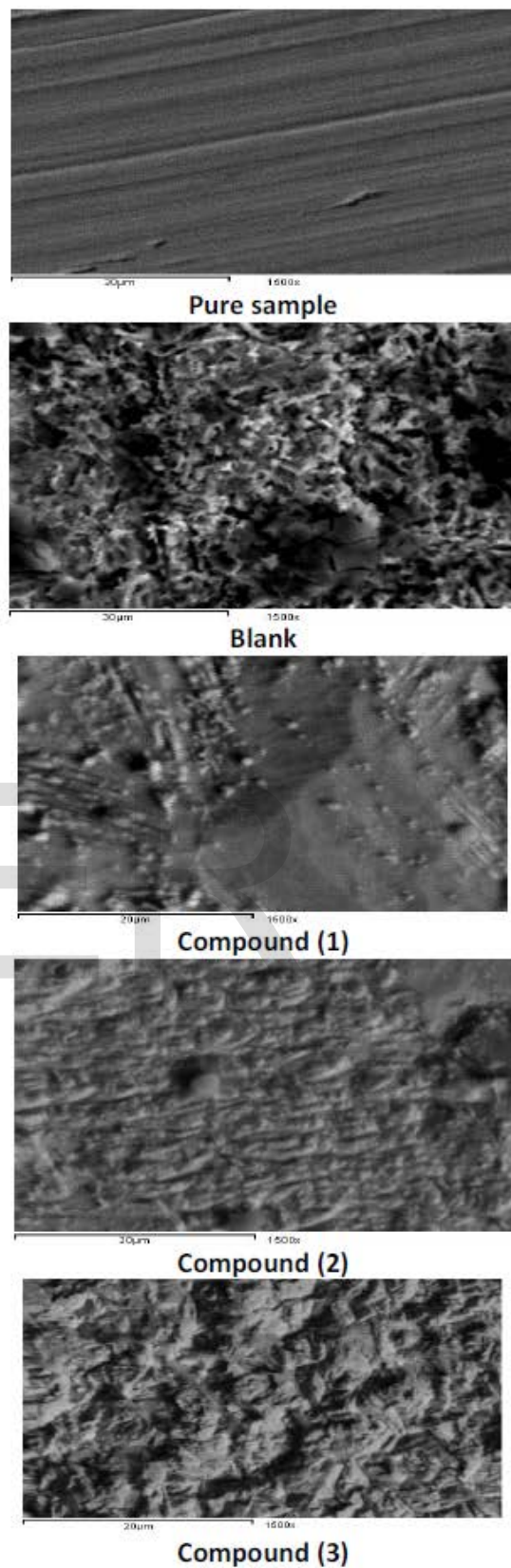
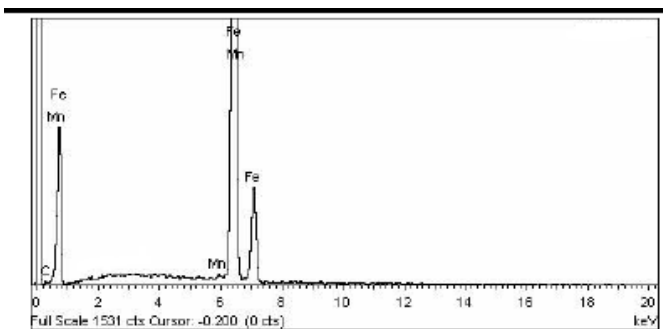
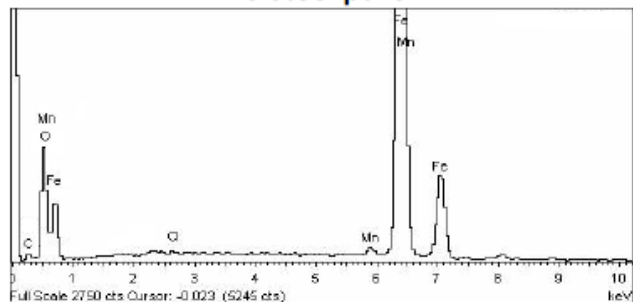


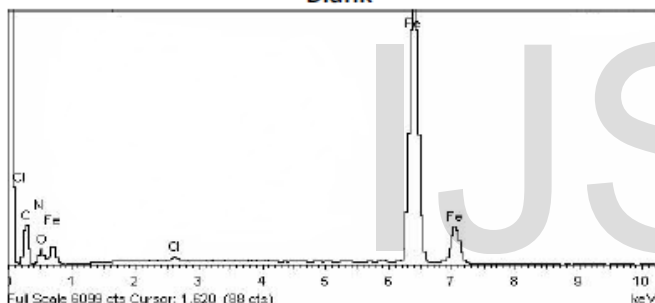
Fig. 15. SEM micrographs for C-steel in the absence and presence of  $11 \times 10^{-6}$  M of nicotinonitrile derivatives after immersion for 3 days.



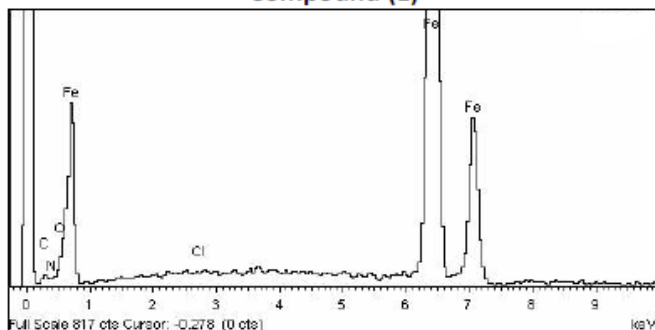
**C-steel pure**



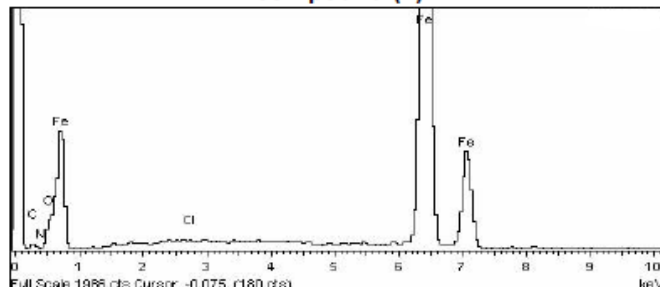
**Blank**



**Compound (1)**



**Compound (2)**



**Compound (3)**

**Fig. 16.** EDS analysis on C-steel in the presence and absence of some nicotinonitrile derivatives for 3 days immersion.

**Table (9):** Surface composition (wt %) of C-steel after 3days of immersion in HCl without and with the optimum concentrations of the studied inhibitors.

(Mass %)	Fe	Mn	C	O	N	Cl
Pure	96.88	0.69	2.43	--	--	--
Blank	65.82	0.64	2.34	28.05	--	0.39
Compound (1)	58.44	0.14	20.44	11.62	7.03	0.10
Compound (2)	60.10	0.11	17.97	13.41	7.03	0.12
Compound (3)	62.52	0.08	15.88	11.92	7.74	0.18

#### 4. Chemical Structure of the Inhibitors and Corrosion Inhibition.

Inhibition of the corrosion of C-steel in 2M HCl solution by some nicotinonitrile compounds is determined by weight loss, potentiodynamic anodic polarization measurements, Electrochemical Impedance Spectroscopy (EIS), electrochemical frequency modulation method (EFM) and Scanning Electron Microscopy (SEM) Studies, it was found that the inhibition efficiency depends on concentration, nature of metal, the mode of adsorption of the inhibitors and surface conditions.

The observed corrosion data in presence of these inhibitors, namely:

The decrease of corrosion rate and corrosion current with increase in concentration of the inhibitor.

The linear variation of weight loss with time.

The shift in Tafel lines to higher potential regions.

The decrease in corrosion inhibition with increasing temperature indicates that desorption of the adsorbed inhibitor molecules takes place.

The inhibition efficiency was shown to depend on the number of adsorption active centers in the molecule and their charge density.

It was concluded that the mode of adsorption depends on the affinity of the metal towards the  $\pi$ -electron clouds of the ring system. Metals such as Cu and Fe, which have a greater affinity towards aromatic moieties, were found to adsorb benzene rings in a flat orientation. The order of decreasing the percentage inhibition efficiency of the investigated inhibitors in the corrosive solution was as follow:

$$1 > 2 > 3$$

Compound (1) exhibits excellent inhibition power due to: (i) its larger molecular size that may facilitate better surface coverage, and (ii) presence of sulphur atom which is more inhibition than oxygen atom

Compound (2) comes after compound (1) in inhibition efficiency due to its lower molecular size than compound (1).

Compound (3) comes after compound (2) in inhibition efficiency, because it has lower molecular size than compound (2).

#### REFERENCES

[1] Thomas, J.G.N., European Symposium on Corrosion Inhibitors, 5<sup>th</sup> Edn., Ferrara, Italy, 1980.

- [2] Atta, A.M., El-Mahdy, G.A., Ismail, H.S., and Al-Lohedan, H.A., "Effects of Water Soluble Rosin on the Corrosion Inhibition of Carbon Steel," *Int. J. Electrochem. Sci.*, 2012, 7, 11834-11846.
- [3] Manimaran, N., Rajendran, S., Manivannan, M. and John, Mary, S., "Corrosion Inhibition of Carbon Steel by Polyacrylamide," *Research Journal of Chemical Sciences*, 2012, 2, 52-57.
- [4] Subramanyam, N.C., Sheshadri B.S., and Mayanna S.M., Thiourea and substituted thioureas as corrosion inhibitors for aluminium in sodium nitrite solution, *Corro. Sci.*, 1993, 34, 563-571.
- [5] Abd El-Lateef, H.M., Aliyeva, L. I., Abbasov, V. M., and Ismayilov, T. I., "Corrosion inhibition of low carbon steel in CO<sub>2</sub>-saturated solution using Anionic surfactant", *Advances in Applied Science Research*, 2012, 3, 1185-1201.
- [6] Fouda, A. S., Mostafa, H. A., El-Taib Haekel, F., and Elewady, G. Y., "Synergistic influence of iodide ions on the inhibition of corrosion of C-steel in sulphuric acid by some aliphatic amines," *Corro. Sci.*, 2005, 47, 1988-2004.
- [7] Yurchenko, R., Pogrebova, L., Pilipenko, T., and Shubina, T., "Anticorrosive properties of N-acetylmethylpyridinium bromides", *Russian J. Appl. Chem.*, 79, 2006, 1100-1104.
- [8] Heikal, F.T., Fouda, A.S., and Radwan, M.S., "Inhibitive effect of some thiadiazole derivatives on C-steel corrosion in neutral sodium sodium chloride solution," *Mater.Chem. Phys.*, 2011, 125, 26-36.
- [9] Abdallah, M., Asghar, B.H., Zaafarani, I., and Fouda, A.S., "The inhibition of carbon steel corrosion in hydrochloric acid solution using some phenolic compounds," *Int. J. Electrochem. Sci.*, 2012, 7, 282-304.
- [10] Fouda, A.S., El-Desoky, A.M., and Al-Sarawy, A.A., "Some hydrazide derivatives as inhibitors for the corrosion of Zn in NaOH solution," *J. Corro. Sci. & Technol.*, 2005, 7, 30-36.
- [11] Singh, A.K., Shukla, S.K., Quraishi, M.A., and Ebenso, E.E., "Investigation of adsorption characteristics of N,N'-(methylimino)dimethyldiyl-di-2,4-xylylene as corrosion inhibitor at mild steel/sulphuric acid interface," *J. Taiwan Institute of Chem. Engin.*, 2012, 43, 463-472.
- [12] Bentiss, F., Lagrenee, M., Traisnel, M., and Hornez, J.C., "The corrosion inhibition of mild steel in acidic media by a new triazole derivative," *Corro. Sci.*, 1999, 41,789-803.
- [13] Nagiub, A.M., Mahross, M.H., Khalil, H.F.Y., Mahran, B.N.A., Yehia, M.M., and El-Sabbah, M.M.B., "Azo Dye Compounds as Corrosion Inhibitors for Dissolution of Mild Steel in Hydrochloric Acid Solution," *Portugal. Electrochim. Acta* 2013, 31, 119-139.
- [14] Orhan, A., Ercan, D., Koparir, P., and Soylemez, A., "Corrosion Inhibition of Mild Steel by 4-Allyl-5-pyridin-4-yl-4H-1,2,4-triazole-3-thiol," *Chem. Sci. Trans.*, 2012, 1, 463-469.
- [15] Aramaki, K., Hagiwara, M., and Nishihara, H., The synergistic effect of anions and the ammonium cation on the inhibition of iron corrosion in acid solution, *Corro. Sci.*, 1987, 27, 487-497.
- [16] Subramanyam, N.C., Mayanna, S.M., "Azoles as corrosion inhibitors for mild steel in alkaline mine water, *Corro. Sci.*, 1985, 25, 163-169.
- [17] Fouda, A.S., Heikal, F. T., and Radwan, M.S., "Role of some thiazole derivatives as inhibitors for the corrosion of C-steel in H<sub>2</sub>SO<sub>4</sub>," *J. appl. electrochem.*, 2009, 39, 391-402.
- [18] Abdallah, M., helal, E.A., and Fouda, A.S., "Some aromatic hydrazone derivatives as inhibitors for the corrosion of C steel in H<sub>3</sub>PO<sub>4</sub> solution," *Ann. Chim.*, 2006, 96, 85-96.
- [19] Aramaki, K., and Hackerman, N., "Inhibition Mechanism of Medium-Sized Polymethyleneimine," *J. Electrochem. Soc.*, 1969, 116, 568-574.
- [20] Kissi, M., Bouklah, M., Hammouti, B., Benkaddour, M., Establishment of equivalent circuits from electrochemical impedance spectroscopy study of corrosion inhibition of steel by pyrazine in sulphuric acidic solution, *Appl. Surface Sci.*, 2006, 252, 4190-4197.
- [21] Li, X., Deng, S., Fu, H., and Mu, G., "Inhibition effect of 6-benzylaminopurine on the corrosion of cold rolled steel in H<sub>2</sub>SO<sub>4</sub> solution", *Corro. Sci.*, 2009, 51,620-634
- [22] Fouda, A.S., El-desoky, A.M., and Ead, D.M., "Anhydride Derivatives as Corrosion Inhibitors for Carbon Steel in Hydrochloric Acid Solutions," *Int. J. Electrochem. Sci.*, 2013, 8, 8823- 8847.
- [23] Abdel-Rehim, S.S., Khaled, K.F., and Abd-Elshafi, N.S., Electrochemical frequency modulation as a new technique for monitoring corrosion inhibition of iron in acid media by new thiourea derivative, *Electrochim. Acta*, 2006, 51, 3269-3277.
- [24] Elewady, G.Y., El-Said, I.A., and Fouda, A.S., "Anion surfactants as corrosion inhibitors for Al dissolution in HCl solutions," *Int. J. Electrochem. Sci.*, 2008, 3, 177-190.
- [25] Abd El-Rehim, S.S., Refaey, S.A.M., Taha, F., Saleh, M.B., and Ahmed, R.A., Corrosion inhibition of mild steel in acidic medium using 2-amino thiophenol and 2-cyanomethyl benzothiazole, *J. Appl. Electrochem.*, 2001, 31, 429-435.
- [26] Abd El-Rehim, S.S., Ibrahim, M.A.M., and Khaled, K.F., "4-Aminoantipyrine as an inhibitor of mild steel corrosion in HCl solution," *J. Appl. Electrochem.*, 1999, 29, 429-435.
- [27] Al-Neami, K. K., Mohamed, A. K., Kenawy, I. M., and Fouda, A.S., "Inhibition of the corrosion of iron by oxygen and nitrogen containing compounds," *Monatsh. Chem.* 1995, 126, 369-376.
- [28] Abd El-Rehim, S.S., Refaey, S.A.M., Taha, F., Saleh, M.B., and Ahmed, R.A., "Corrosion Inhibition of Mild Steel in Acidic Medium using 2-amino Thiophenol and 2-Cyanomethyl Benzothiazole," *J. Appl. Electrochem.*, 2001, 31, 429-435.
- [29] Fouda, A.S., Al-Sarawy, A.A., and El-Katori, E.E., "Potentiometric and thermodynamic studies of 3-methyl-phenyl-[p-(pyrimidin-2-yl)sulfamoyl]-phenylazo]-2-pyrazolin-5-one and its metal complexes," *Chem. Paper*, 2006, 60, 5-9.
- [30] Fouda, A.S., EL-Haddad, M.N., "Corrosion inhibition and adsorption behaviour of some azo dye derivatives on carbon steel in acidic medium: synergistic effect of halide ions," *J. Chem. Engineer. Commun.*, ID: 746675, DOI: 10.1080/00986445, Accepted (2013).
- [31] Loto, R.T., Loto, C.A., and Popoola, A.P.I., "Corrosion inhibition of thiourea and thiadiazole derivatives : A Review", *J. Mater. Environ. Sci.*, 2012, 3, 885-894.
- [32] Mansfeld, F., Kendig, M.W., and Tsai, S., "Recording and Analysis of AC Impedance Data for Corrosion Studies", *Corro*, 1982, 38, 570-580.
- [33] Mansfeld, F., Chen, C., Lee, C.C., and Xiao, H., "The effect of asymmetric electrodes on the analysis of electrochemical impedance and noise data " *Corros. Sci.*, 1996, 38, 497-513.
- [34] Nagiub, A., and Mansfeld, F., "Evaluation of corrosion inhibition of brass in chloride media using EIS and ENA," *Corro. Sci.*, 2001, 43, 2147-2171.
- [35] McCafferty, E., and Hackerman, N., Double Layer Capacitance of Iron and Corrosion Inhibition with Polymethylene Diamines, *J. Electrochem. Soc.*, 1972, 119, 146-154.
- [36] Kus, E., and Mansfeld, F., An evaluation of the electrochemical frequency modulation (EFM) technique, *Corro. Sci.*, 2006, 48, 965-979.
- [37] McCafferty, E., "Standard electrode potentials of the elements as a fundamental periodic property of atomic number," *Electrochim. Acta*, 2007, 52, 5884-5890.
- [38] Abdallah, M., Fouda, A.S., SHama, S.A., and Afifi, E.A., "Azodyes as Corrosion inhibitors for dissolution of C-steel in HCl solution," *African J. of pure and appli. Chem.*, 2008, 2, 83-91.
- [39] Fouda, A.S., Abdallah, M., and Attia, A., "Inhibition of C-steel corrosion by some cyanoacetohydride derivatives in HCl solution," *Chem. Eng. Commun.*, 2010, 197, 1091-1108.
- [40] Fouda, A.S., and Elattar, K.M., "Corrosion inhibition of carbon steel by new enamionitrile derivatives in HCl solution," *J. of Scientific & In-*

*dustrial Research*, 2012, 71, 690-698.

IJSER